

Introduction

Stage 2 of the Sectoral Plan for Deep Geological Repositories, developed by the Swiss Federal Office of Energy (SFOE, 2008), aims at selecting one or more sites for the disposal of low/ intermediate level (L/ILW) and high level (HLW) radioactive waste in Switzerland. As a decision basis, so-called provisional safety analyses are to be elaborated. These analyses are an input for the qualitative and quantitative comparison of the long-term safety conditions after closure of the proposed repository configurations in the candidate siting regions. The present study focuses on the temporal evolution of hydraulic parameters of the Excavation Damage Zone (EDZ hereinafter) around the gallery. To that end, a hybrid finite/discrete element method (FEMDEM) was first used to simulate the geometry and geomechanical conditions of discrete fracture networks forming the EDZ, which develop in response to the excavation process in the rock mass around the underground structures of a radioactive waste repository (NAGRA, 2013). The geometry and geomechanical properties simulated at that stage are mapped onto a finite element mesh, which allows us to solve the fluid motion equations at the near-field.

The objectives of this study are:

- 1) To quantify the temporal evolution of hydraulic properties in response to pressure variations caused by the resaturation of the EDZ after excavation and emplacement.
- 2) To quantify the temporal evolution of the specific axial flux through the EDZ.
- 3) To quantify the total time required for a full resaturation of the EDZ.

This paper is organized as follows. First, the methodology is succinctly described. Second, an application to one of the repository configurations is presented. The paper ends with some recommendations for future work.

Method and/or Theory

1) Basic input and pre-processing

The starting point of our methodology is a fracture network simulated by a hybrid finite/discrete element method (FEMDEM; NAGRA, 2013). Apertures and fracture lengths are calculated from the 4-node geometrical definition of the fracture patches. Fracture aperture is used to infer fracture transmissivity through the cubic law. Figure 1 displays the geometry of the fracture network and the transmissivity and aperture distributions.

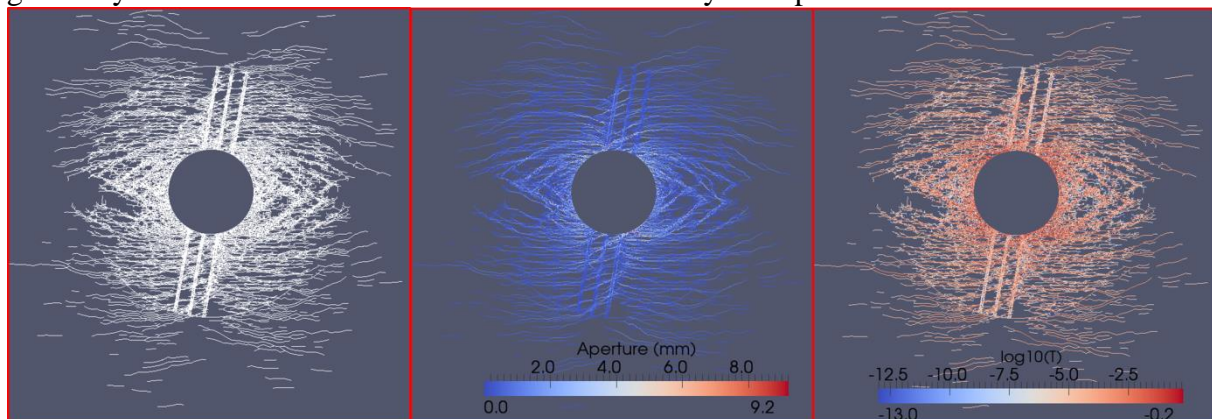


Figure 1. From left to right, (a) fracture network geometry, (b) fracture aperture and (c) fracture transmissivity, inferred from aperture through the cubic law.

2) Mapping discrete fracture properties onto a finite element mesh

At a certain finite element, total porosity and hydraulic conductivity K are a composite of matrix (denoted by sub-index ‘m’) and fracture properties (sub-index ‘f’). Assuming that the total cell porosity ϕ does not vary in time:

$$\begin{aligned}\phi &= \phi_f(t) + (1 - \phi_f(t)) \phi_m(t) \\ K(t) &= K_f(t) + K_m(t)\end{aligned}\tag{1}$$

Fracture porosity and hydraulic conductivity are inferred from the discrete properties in Figure 1 and the following upscaling laws:

$$K_f = \frac{\sum_i T_i L_i}{V_{tot}}\tag{2}$$

$$\phi_f = \frac{\sum_i b_i L_i}{V_{tot}}$$

where b_i and L_i are the aperture and trace length of a fracture ‘ i ’ intersecting the finite element. Figure 2 displays the initial hydraulic conductivity and porosity, as inferred from the input fracture network.

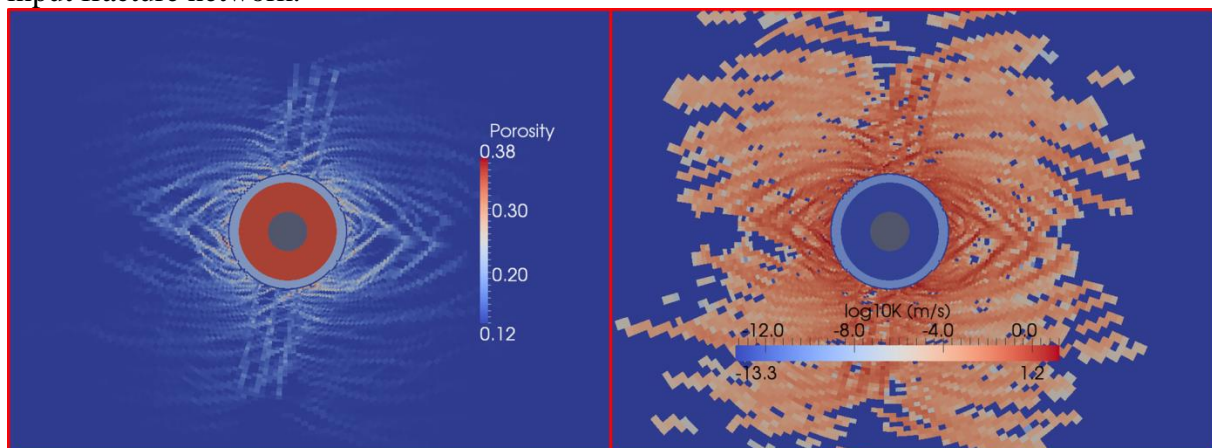


Figure 2. Initial spatial distribution of porosity (left) and hydraulic conductivity (right).

3) Temporal variation of hydraulic properties caused by the resaturation of the EDZ

The resaturation of the EDZ causes a pore pressure increase at that zone. This leads to a decrease of the normal effective stress and, correspondingly, to the progressive closure of the fracture. Bandis et al. (1983) introduced a simple hyperbolic model for a single fracture, expressing the aperture b as a function of effective normal stress σ'_n on the fracture plane:

$$b(t) = b_0 - \frac{\sigma'_n}{b_0 K_{n0} + \sigma'_n}\tag{3}$$

where b_0 is the initial aperture (see Figure 1b) and K_{n0} is fracture normal stiffness. Fracture porosity is calculated from fracture aperture (equation 2). Assuming that the total porosity is constant along the process and plugging $\phi_f(t)$ in equation (1.1) allows us to obtain the spatial distribution of matrix porosity $\phi_m(t)$. Matrix porosity and hydraulic conductivity can be related through the well-known Kozeny-Carman law:

$$K_m(t) = \frac{\phi_m(t)^3}{(1 - \phi_m(t))^2} \cdot \frac{\rho \cdot g}{\mu} \cdot \frac{d_{10}^2}{180} \quad (4)$$

where ρ and μ are fluid density and viscosity, respectively and d_{10} is the particle size for which 10% of the soil is finer.

Equation (3) can also be plugged in the cubic law to render the temporal evolution of fracture transmissivity $T_f(t)$. Revisiting mesh elements intersected by fractures and applying the upscaling laws in equation (2) allows us to obtain a new spatial distribution of the anisotropic hydraulic conductivity field at time t .

Results

Transient resaturation with variable hydraulic properties is simulated over a total period of 10'000 years. Boundary conditions are hydrostatic. Initial conditions are fully saturated, the initial pressures being hydrostatic everywhere but at the EDZ and buffer zones, where atmospheric pressure is applied. Screenshots of pressure and hydraulic conductivity are displayed in Figure 3. As observed, the resaturation is very fast at the beginning and very slow at late times.

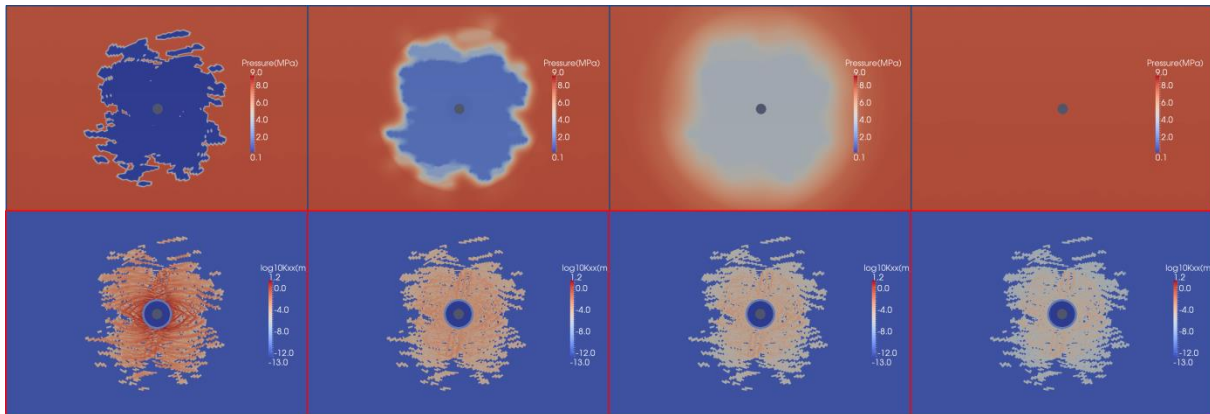


Figure 3. Temporal evolution of pressure (upper panels) and hydraulic conductivity. From left to right, calculation times are: $t=0$ years, $t=0.5$ years, $t=10$ years and $t=8'700$ years (full resaturation).

The spatio-temporal evolution of hydraulic properties is also used to derive a simplified model including homogeneous step-wise zonation and to calculate the specific axial flux across the vertical section (Figure 4). As observed, the extent of the EDZ is about 4.5 meters only. The equivalent axial conductance is obtained through upscaling of the axial conductances of cells within that radius. In this case, the equivalent initial conductance of the EDZ is 0.11 m/s. This value is indeed very high because initial axial conductances are also very high (see Figure 3a). As observed in Figure 3, the equivalent conductance will drop substantially during the first 10 years. Correspondingly, the axial specific flux will drop to an almost negligible value.

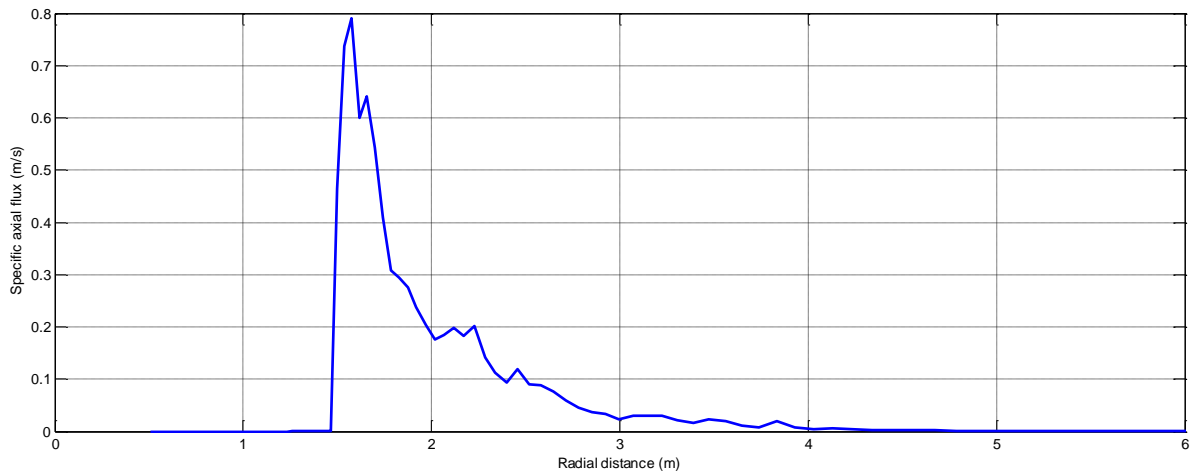


Figure 4. Spatial distribution of the specific axial flux across a vertical section at time $t=0$ years.

Future work

The results presented here assume saturated conditions of the buffer zone. Next steps consist of:

- 1) Assuming unsaturated conditions. This will make the total resaturation time to increase substantially.
- 2) Analyzing the impact of the geometry of the gallery and the EDZ.
- 3) Simulating bi-phase flow of water and gas.
- 4) Stochastic modeling of the EDZ.

References

- Bandis S.C., Lumsden A.C., Barton N.R. (1983). Fundamentals of rock joint deformation. Int. J. Rock. Mech. Min. Sci. and Geomech. Abstr. V20(6), pp. 249-268.
- Nagra (2013). NAB 13-78. Extent and shape of the EDZ around underground structures of a geological repository for radioactive waste – A sensitivity study for the candidate host rocks in the proposed siting regions in Northern Switzerland
- Swiss Federal Office of Energy (SFOE; 2008). Sectoral Plan for Deep Geological Repositories, Conceptual Part. Swiss Federal Office of Energy, Bern, Switzerland.